Effect of 3.0 wt% Indium doping on ethanol sensing properties of nanocrystalline Bi_2O_3

S. D. Kapse [*]

Department of Physics, G. S. College, Khamgaon 444303, Maharashtra, India
ssk.nano@gmail.com

ABSTRACT

Nanocrystalline powders of pure and 3.0 wt% indium doped Bismuth oxide (Bi_2O_3) were prepared by ethyl alcohol mediated decomposition route. The prepared samples were then characterized in order to investigate the structural, electrical and reducing gas sensing properties of pure and In doped Bismuth oxide. X-ray diffraction (XRD) was used to confirm the material structure and transmission electron microscopy (TEM) to depict the crystallite microstructure. Bismuth oxide based thick films were expose to study the conductance response of different reducing gases such as like liquefied petroleum (LPG), ammonia (NH_3), hydrogen sulfide (H_2S), and ethanol gas (C_2H_5OH) etc. The sensor exhibited various sensing responses to these gases at different operating temperatures. From result it is found that 3.0 wt% In-doped Bi_2O_3 shows the maximum response to 50 ppm ethanol at 260 ^{0}C also fast response and good recovery are the main features of investigated sensors.

Keywords: Nanostructured; Bismuth oxide; Ethanol gas; Dopant; Response time

1. INTRODUCTION

The change in electrical properties of a semiconducting material is because of adsorption and/or reaction with the gases in the atmosphere. This property of semiconducting materials is typically exploited in gas sensing measurements. Semiconducting oxides such as ZnO, TiO_2, Fe_2O_3, WO_3, and SnO_2 are commonly investigated materials for gas sensing applications. The gas sensing properties of these materials are known to be influenced by the material formulation, precursor raw materials, as well as various fabrication and processing conditions that affect the microstructure of the precursor powders and the gas sensing elements. Binary n-type semiconducting oxides (as SnO_2, In_2O_3 or ZnO) have been extensively studied as gas-sensing materials, whereas little has been done in the field of p-type semiconducting oxides for application in gas sensors. Bi_2O_3 is an important metal-oxide semiconductor with a direct band gap 2.85 and 2.58 eV for the monoclinic α- Bi_2O_3 and tetragonal β- Bi_2O_3 phases, respectively [1,2]. Generally Bi2O3 is taken as model for p-type semiconduction Bi_2O_3 appears in four polymorphic modifications denoted as α-, β-, γ - and δ- Bi_2O_3 [3-5]. Structural characterization of all modifications is carried out and their powder diffraction patterns have been discussed [6–13]. Particles of nanosize generally exhibit properties different from their bulk counterparts in regard of electrical, optical and fast-ion conducting characteristics. Because of this nanocrystline Bi_2O_3 material find variety of applications including solid-state electrolytes, superconductors, gas sensors, catalysts, electrical ceramics, [14-20]. Several chemical methods have been used to prepare Bi_2O_3 nanoparticles, e.g. precipitation [20,21], flame spray pyrolysis [22], and sol–gel methods [23]. It is well know that the gas sensing properties depend naturally on the catalytic or surface chemical properties of sensing materials used, beside their physical or morphological properties such as grain size, porosity and thickness. This has provided a base on which the gas sensing properties have been modified often significantly by the adding up foreign materials to the sensing materials [24]. In fact, many sensors, which are sensitive and selective to particular gases, have been developed through such modification techniques. Bi_2O_3 in combination with other typically used metal oxide, such as SnO_2 [25], Nb_2O_5 [26], and WO_3 [27], was studied as a useful sensitive material for detecting CO, H_2, and NO gas, respectively. The tungsten-stabilized Bi_2O_3 solid electrolyte has been studied as a sensitive material for CO_2 gas sensors [28]. It has been proposed that the Bi_2O_3 is a highly selective oxide for NO detection in front of the NO_2 as interfering species [22].

From the literature survey it is observed that there are very rare reports on ethanol sensing properties of pure and indium doped Bi_2O_3. Thus by considering this the present paper focused on the synthesis of nanocrystalline Bi_2O_3 by thermal decomposition route in the aqueous medium of ethyl alcohol. Further, the influence of indium doping on the structural, morphological, electrical and ethanol gas sensing properties of Bi_2O_3 were also investigated.

2. Experimental

2.1 Synthesis of nanocrystalline pure and doped Bi_2O_3 powders

Appropriate quantity of bismuth nitrate [Bi $(NO_3)_3 \cdot H_2O$] was grounded for 30 min. in an agate mortar pestle and then mixed with absolute ethanol. The mixture was vigorously stirred for ~2 hours at 70 ^{0}C temperature and then the suspension was transferred into a Teflon lined stainless steel autoclave. The temperature of the autoclave was raised slowly to 170 ^{0}C and maintained for 10 h. Thereafter, the autoclave was allowed to cool naturally to room temperature and the resulting product washed several times with deionized water and absolute ethanol to remove the possible residue. Then the product was kept for drying overnight at 100 ^{0}C in an oven, which was followed by calcination at 600 ^{0}C and for 6 h. Depending on the required In doping concentration [In $(NO_3)_3 \cdot H_2O$] was added separately to the mixture of bismuth nitrate and absolute ethanol. The calcined materials were then grounded into fine powders, sieved and dispersed with a temporary binder as a mixture of organic solvents to form pastes in order to study gas sensing properties. For formulating the paste the ratio of inorganic to organic part was kept as 75:25. The thick films are prepared on glass substrate using

screen printed method from the paste. The films prepared were fired at 500 ^{0}C for 2 h. For measurement of electrical properties the silver contacts were developed by vacuum evaporation method. The thicknesses of the films were observed to be in the range from 25 to 30 μm.

Further the pure and 3.0% In doped $B_{i2}O_3$ were the characterization usind different techniques . The crystal phases of calcined samples were analyzed using X-ray diffraction (XRD), (Model: Philips X'pert) with copper target, K_α radiation (λ = 1.54059 Å). The morphologies of the synthesized powder were observed through a transmission electron microscopy (TEM), (Model: Philips CM 200). FT-IR spectra were obtained on Magna 560 FT-IR spectrometer with a KBr disk. The 'static gas-sensing system' is employed for studying the performance of the sensors. The details of sensor assembly and the circuitry for the sensor characteristics measurement was reported in our earlier publication [29]. The response time is the time taken by the sensor to attain the maximum (90%) change in conductance on exposure to the target gas and the recovery time is the time taken by the sensor to get back 90% of the original conductance.

3. RESULTS AND DISCUSSION

3.1 Material characterizations

Generally Bismuth oxide exists in four phases, two stable (monoclinic α -Bi_2O_3 and cubic-Bi_2O_3) and two metastable (tetragonal β -Bi_2O_3 and bcc γ-Bi_2O_3), which are interconvertable at certain condition [23]. In all cases, the forms strongly depend on the synthesis method. Figure 1(a) and (b) shows the XRD pattern of pure and 3.0 wt% In-doped Bi_2O_3, calcinated at 600 ^{0}C and for 6 h. Intense and sharp peaks confirms the high degree of crystallinity of powder. From figure all diffraction peaks are assigned to bismite crystallized in monoclinic form (α-Bi_2O_3) corresponding to JCPDS Card No. 01-072-0398. For the pure Bi_2O_3, only α- Bi_2O_3 phase was detected after cooling down to room temperature. XRD patterns confirms that the Bi_2O_3 has only monoclinic α- Bi_2O_3 phase while 3.0 wt% In-doped Bi_2O_3 has mixture of monoclinic α-Bi_2O_3 along with the traces of non-stiochiometric $Bi_2O_{2.33.}$ The introduction of additional phase after In-doping gives good agreement with earlier report by Cabot [22].
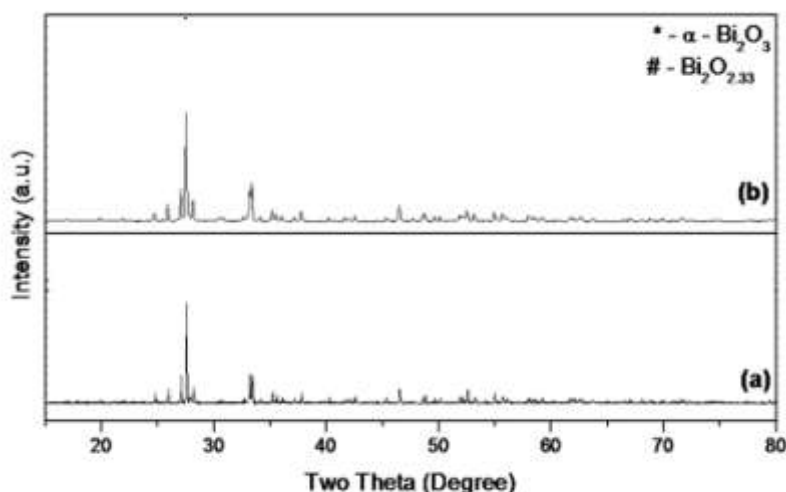

Fig. 1: XRD patterns of (a) pure Bi_2O_3 and (b) 3.0 wt% In-doped Bi_2O_3 calcinated at 600 ^{0}C.

The crystalline pattern of powders and the observed d-lines match the reported values for α-Bi_2O_3 phase. The average crystallite size has been calculated from the XRD peaks using Debye-Scherrer formula. The calculated average crystallite size and lattice parameters of the synthesized powder are illustrated in Table 1. The good agreement between calculated lattice parameters by least squares method and literature data reported for α - Bi_2O_3 phase confirms that the synthesized powders are monoclinic Bi_2O_3 nanocrystallites.

Table 1: Summary of the crystallite size, the calculated lattice parameters of the synthesized samples.

Sample	Average crystallite size (nm)	Calculated lattice parameters (Å)	α = β= γ [^{o}]	Cell Volume Å^3
Pure Bi_2O_3	16	a = 5.830(5) b = 8.145(4) c = 7.477(5)	α = 90 β= 67.18(1) γ= 90	327.27
Bi_2O_3: 3.0 wt% In	14	a = 5.830(4) b = 8.156(4) c = 7.481(4)	α = 90 β= 67.208(8) γ= 90	327.96

4376 | P a g e
O c t o b e r   2 0 1 6
w w w . c i r w o r l d . c o m

I S S N 2 3 4 7 - 3 4 8 7
V o l u m e 1 2 N u m b e r 3
J o u r n a l o f A d v a n c e s i n P h y s i c s

The TEM image along with selected area electron diffraction (SAED) pattern of the pure and In-dpoed Bi_2O_3 powder samples is depicted in Fig. 2 (a) and (b) respectively. The particles are of spherical in shape and the average particle size varies from 10 nm to 20 nm, which is in good agreement with the XRD result. The well defined SEAD pattern clearly shows the diffraction spots representing different lattice planes of α-Bi_2O_3. The TEM images confirms that Bi_2O_3 nanoparticles are well dispersed and irregular in shape.

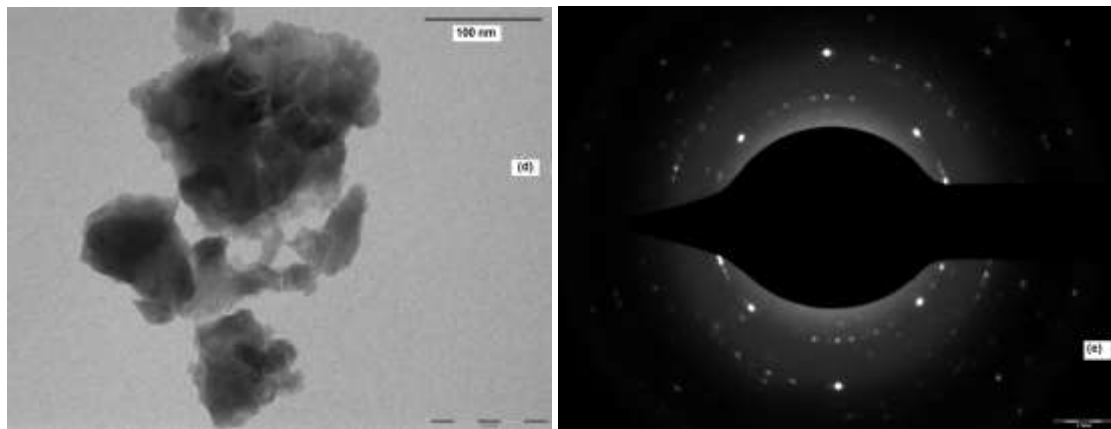**Fig 2 : (a) TEM images of 3.0 wt% In-doped Bi_2O_3 calcinated at 600 ^{0}C (b) Selected area diffraction pattern of 3.0 wt% In-doped Bi_2O_3 calcinated at 600 ^{0}C**
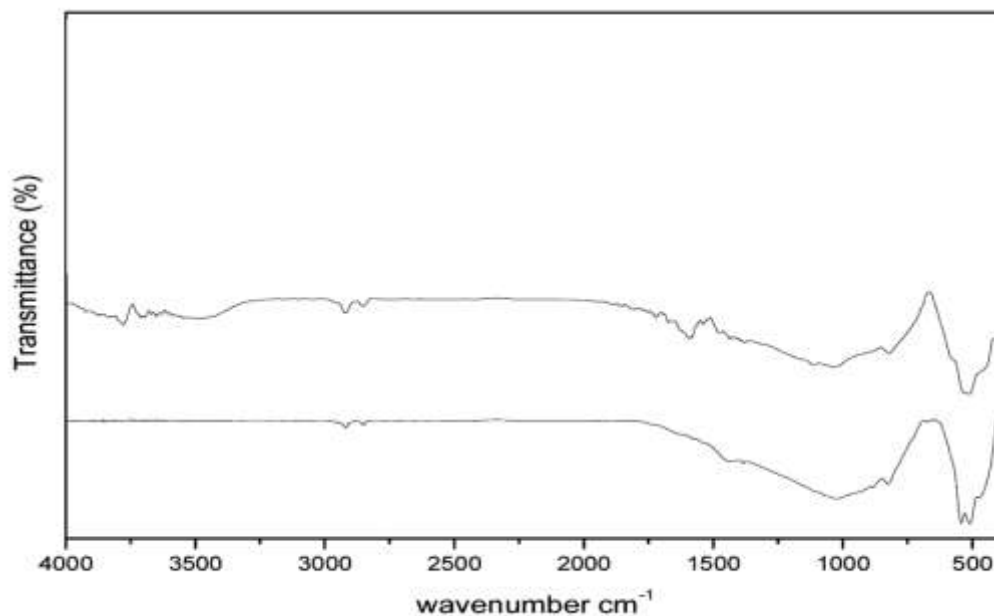
3.2 Fourier transform infrared spectroscopy (FT-IR):

Fig. 3: FTIR spectra of (a) pure Bi_2O_3, (b) 3.0 wt% In-doped Bi_2O_3 calcinated at 600 ^{0}C.

Fig. 3 depicts the IR spectra of the pure and 3wt% of Bi_2O_3 samples calcinated at 600 ^{0}C. From figure a strong absorption band appeared in the 544.00–443.00 cm^{-1} range is due to Bi–O stretching and deformation mode [30]. In addition to this there is also the absorption band appeared at about 443.00, 509.00 and 543.00 cm^{-1} in FTIR spectra can be assigned to α-Bi_2O_3 [31]. Furthermore, a systematically shift of the bands was observed, suggesting a possible substitution of Bi^{3+} by dopand ions. Changing the substituted ions in the samples led to slightly different features in the IR spectra. These findings are in agreement with XRD diffractogram results. Besides, it needs to mention that an absorption band at about 1060 cm^{-1} is also observed. As organic molecules are removed completely, this absorption band may be attributed to the other kinds of vibrations of Bi–O caused by the interaction between the Bi–O bonds and their other surroundings [32].

3.3 D.C Electrical conductivity measurements

The effect of 3.0 wt% In doping on dc electrical conductivity (σ) have been suited by ethanol mediated decomposition route. The two-probe method was used to study the dc electrical conductivity of Bi_2O_3 based thick films as a function of temperature in the range 323–623 K. The variation of the log σ with 1000/T is shown in Fig. 4 which confirm semiconducting nature of pure and 3.0 wt% In-doped Bi_2O_3 materials. It is observed that the log σ vs. 10^3/T curves present

I S S N 2 3 4 7 - 3 4 8 7
V o l u m e 1 2 N u m b e r 3
J o u r n a l o f A d v a n c e s i n P h y s i c s

almost two regimes. The first one, in the lower temperature range (323 K < T1 < 433 K), is characterized by a smaller slope. The next portion in the higher temperature range (433 K < T2 < 623 K) is characterized by larger slope where the intrinsic conduction probably prevails.
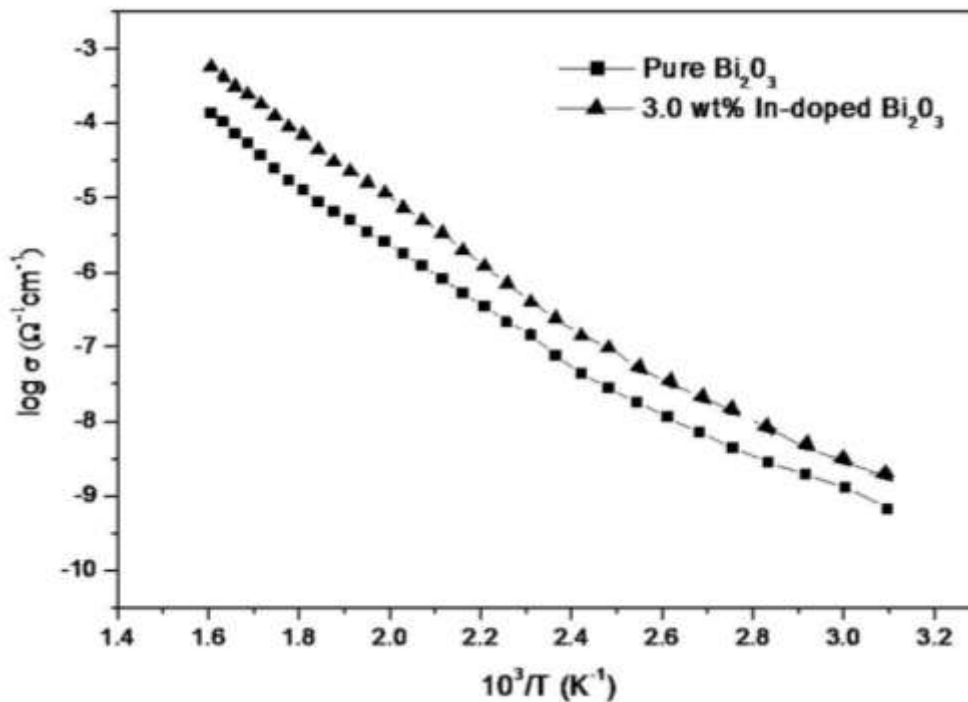
**Fig. 4: Variation of log (σ) versus $10^3/T$ for pure and In-doped bismuth oxide thick films.**

The table 2 represents the activation energies obtained from the slope of the log σ vs. 1000/T plot. The predominance of grain boundary scattering is responsible for low activation energy in the lower temperature regime. However, at higher temperatures, the position of trap levels in the semiconductor forbidden band towards the lower limit of the conduction band leading to increase in activation energy. The Gujar et al. reported the existence of different activation energies in lower and higher temperature domains [33].

| Sample	$(\Delta E_a)_{HT}$ eV	$(\Delta E_a)_{LT}$ eV
Pure Bi_2O_3	0.83	0.48
3.0 wt% In -doped Bi_2O_3	0.83	0.56

Table 2 : The experimental values of activation energies $(\Delta E_a)_{HT}$ and $(\Delta E_a)_{LT}$ (eV)

3.4 Gas sensing studies of nanocrystalline pure and 3.0 wt% In-doped Bi_2O_3:

Fig. 5. illustrated the response of pure Bi_2O_3 based sensor element as a function of operating temperature towards H_2, NH_3, CO_2, H_2S, LPG and ethanol. From figure it is observed that the sensor response for each test gas changes with operating temperature. It increases with increase in operating temperature, reaches maximum corresponding to optimum operating temperature and decreases further. The chemical reaction on the surface of the grains and the speed of diffusion of the gas molecules into the surface decides the response of a semiconductor oxide gas sensor to the given gas. These are the activation processes [38]. In the present investigation, the sensor element based on pure Bi_2O_3 exhibited good response towards 50-ppm ethanol at an operating temperature of 300 ^{0}C as compared to other tested gases at the same temperature

4378 | P a g e
O c t o b e r 2 0 1 6
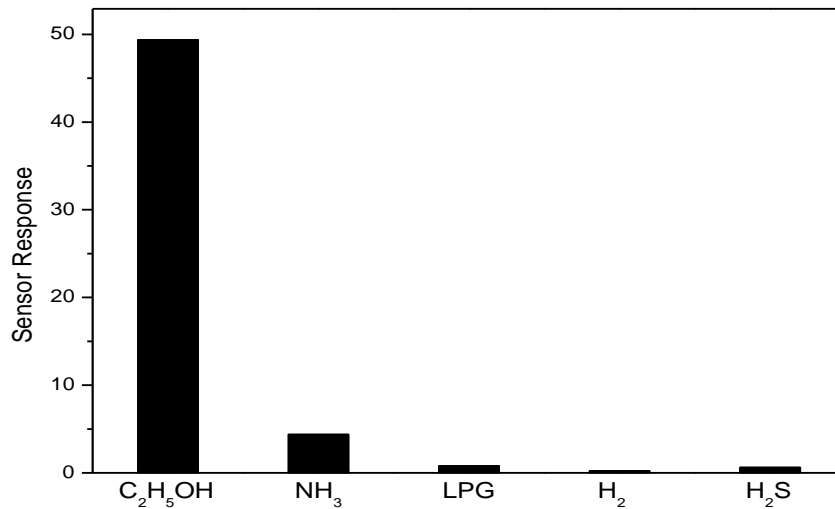w w w . c i r w o r l d . c o m
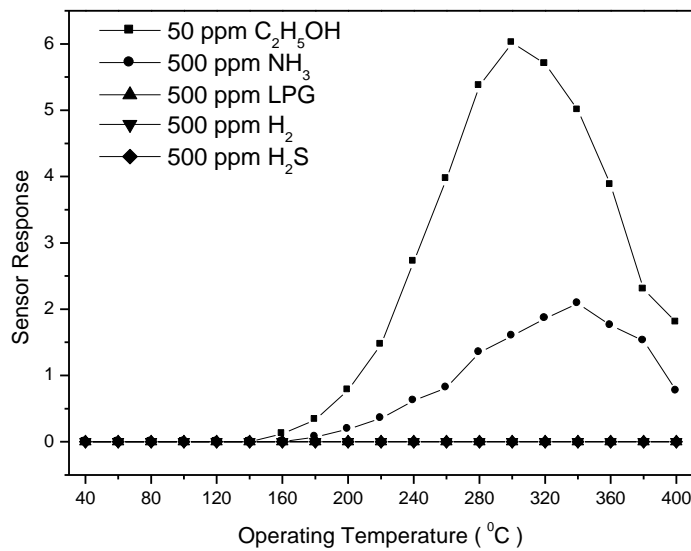
Figure 5: Sensor response of pure Bi$_2$O$_3$ to different reducing gases as a function of operating temperature.


.
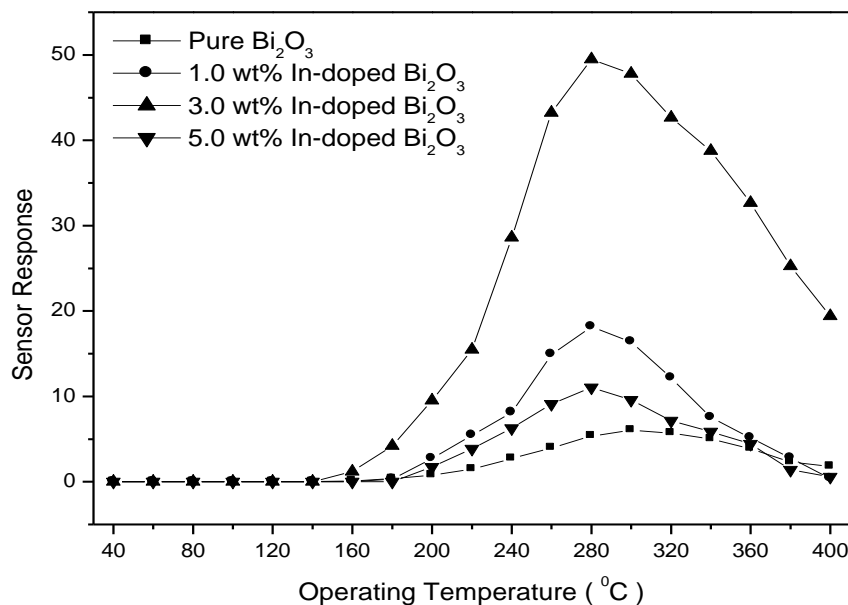
Fig. 6: Sensor response of In-doped Bi$_2$O$_3$ to 50 ppm C$_2$H$_5$OH as a function of operating temperature

Fig.6 shows the effect of of 3.0 wt% In content on ethanol sensing properties of Bi$_2$O$_3$ based sensors. It can be seen that 3.0 wt% In-doped Bi$_2$O$_3$ based sensors have enhanced response towards 50 ppm ethanol vapors than a pure Bi$_2$O$_3$ -based sensor. Further, the optimal operating temperature of In-doped Bi$_2$O$_3$ sensor found to be reduced by 20^{0}C i.e. form 300^{0}C to 280^{0}C and exhibited maximum response of 49.4 towards 50 ppm ethanol. About 8 times increase in the response of 3.0 wt% In-doped Bi$_2$O$_3$ towards ethanol as compared with pure Bi$_2$O$_3$ may also be related to the reduced crystallite size with In doping which results to bigger specific surface and thus cause more oxygen adsorption on the surface. Also presence of non-stiochiometric Bi$_2$O$_{2.33}$ phase along with monoclinic phase and basic nature of In dopant could be another reason for the enhanced response. In case of 3.0 wt% In-doped Bi$_2$O$_3$, the optimum operating temperature reduces to 280^{0}C.

I S S N   2 3 4 7 - 3 4 8 7
V o l u m e   1 2   N u m b e r   3
J o u r n a l   o f   A d v a n c e s   i n   P h y s i c s

Fig. 7: The response vs. C_2H_5OH concentration of 3.0 wt% In-doped Bi_2O_3

The selectivity β is equal to S_1/S_2, where S_1 and S_2 stand for the response in ethanol and other vapors, respectively [51]. Commonly, it is required that β to the ethanol sensor is more than 5 as an ethanol sensor. In order to study the selectivity of the sensor to ethanol vapor, we tested the response of 3.0 wt% In-doped Bi_2O_3-based sensor to LPG, H_2, NH_3 and H_2S (500 ppm each) at 280 ^{0}C. From Fig. 7, , it can be seen that the response to ethanol vapors was much greater than those to other gases, the S value to ethanol is 49.4, while that of LPG, H_2, NH_3, and H_2S is only 0.82, 0.24, 4.38 and 0.64, respectively. For 3.0 wt% In-doped Bi_2O_3 based sensor, the values of β are 60.24, 205.8, 11.2 and 77.1 to LPG, H_2, NH_3, and H_2S respectively. It means that the sensor has very good selectivity to ethanol gas. So, it can be concluded that 3.0 wt% In-doped Bi_2O_3 based sensor elements has very good selectivity to ethanol gas.
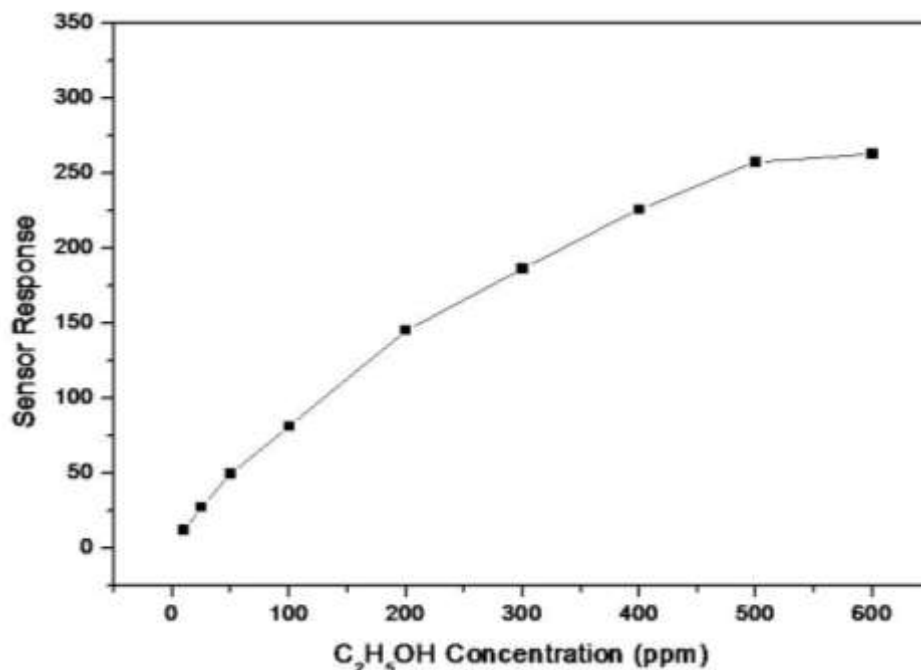
Fig 8:The response vs. C_2H_5OH concentration of 3.0 wt% In-doped Bi_2O_3

Fig. 8 depicts the dependence of the response of 3.0 wt% In-doped Bi_2O_3-based sensors on the concentration of ethanol at 280 ^{0}C. The response to ethanol varies almost linearly up to 500 ppm concentration and afterward it attains saturation level. Thus the 3.0 wt% In-doped Bi_2O_3 based sensors can be a good sensor for testing drinking drivers.
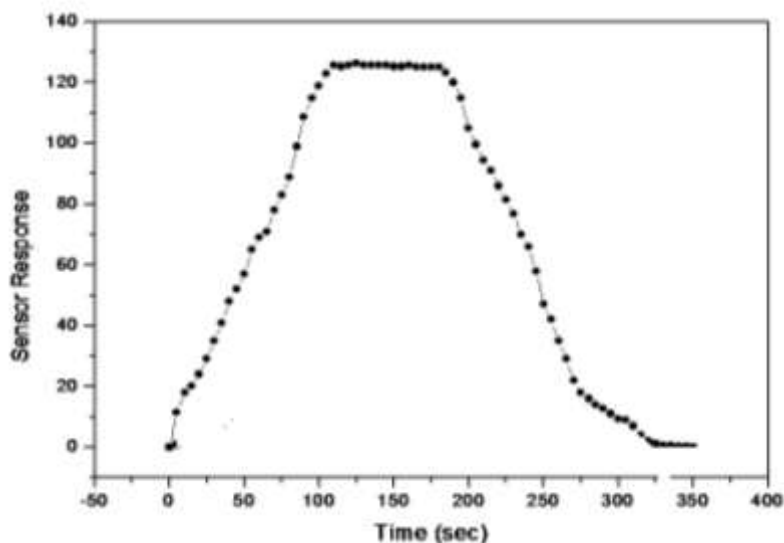
Fig. 9: Response - recovery characteristics of 3.0 wt% In-doped Bi_2O_3 to 50 ppm C_2H_5OH at 280 ^{0}C and 260 ^{0}C respectively

The response-recovery characteristics of 3.0 wt% In-doped Bi2O3 in presence of 50 ppm C2H5OH is presented in Fig. 9. From this figure, it can be noticed that the response and recovery times of 3.0 wt% In-doped Bi2O3 at 280 0C for 50 ppm C2H5OH are 110 and 100 s respectively. Stability is one of the most important characteristics for the sensors. Stability of investigated pure Bi2O3 and 3.0 wt% In-doped Bi2O3 based sensor elements was continuously measured at 300 ^{0}C and 280 ^{0}C for 90 days at an interval of 10 days. We found that sensor response is stable except a small variation. Thus the investigated sensor elements showed good stability and durability.

4. Conclusions

Nanocrystalline pure and 3.0 wt% In-doped Bi_2O_3 powder samples were successfully prepared by ethyl alcohol mediated decomposition route with calcinations at 600 ^{0}C for 4 h. The prepared materials showed p-type semiconducting properties. The sensors based on pure Bi_2O_3 showed good response to 50 ppm C_2H_5OH gas at 300 ^{0}C as compared with other tested reducing gases. 3.0 wt% In -doped Bi_2O_3 exhibited enhanced response to ethanol as compared with pure Bi_2O_3. The sensor based on 3.0 wt% In-doped Bi_2O_3 exhibited large response and good selectivity to ethanol, and good response-concentration linearity at 280 ^{0}C. The enhanced performance of 3.0 wt% In-doped Bi_2O_3 to 50 ppm C_2H_5OH may be attributed to the reduced crystallite size, basic nature of In and mixed phase composition of Bi_2O_3. Also, in addition In could enhance the activity of the surface adsorbed oxygen and make it easy to react with C_2H_5OH. The sensor based on 3.0 wt% In-doped Bi_2O_3 demonstrated fast response (110 s) and recovery (100 s) towards 50 ppm C_2H_5OH at 280 ^{0}C.

4. REFERENCES

1. P. Maruthamuthu, K. Gurunathan, E. Subramanian, Int. J. Hydrogen Energy 19 (1994) 889-893

2. K. Gurunathan, Int. J. Hydrogen Energy 29 (2004) 933 - 940.

3. E.M. Levin, R.S. Roth, J. Res. Natl. Bur. Stand. A 68 (1964) 189 –195

4. E.M. Levin, R.S. Roth, J. Res. Natl. Bur. Stand. A 68 (1964) 197–206.

5. H.A. Harwig, A.G. Gerards, Thermochim. Acta 28 (1979) 121-131

6. H.A. Harwig, Z. Anorg. Allg. Chem. 444 (1978) 151-166

7. G. Malmros, Acta Chem. Scand. 24 (1970) 384-396

8. S.A. Ivanov, R. Tellgren, H. Rondlöf, V.G. Orlov, Powder Diff. 16 (1991) 227-230

9. G. Gattow, D. Schütze, Z. Anorg. Allg. Chem. 328 (1964) 44-68

10. S.K. Blower, C. Greaves, Acta Crystallogr. C 44 (1988) 587-589

11. S.C. Abrahams, P.B. Jamieson, J.L. Bernstein, J. Chem. Phys. 47 (1967) 4034-4041.

12. S.C. Abrahams, J.L. Bernstein, C. Svensson, J. Chem. Phys. 71 (1979) 788-792.

13. J.W. Medernach, R.L. Snyder, J. Am. Ceram. Soc. 61 (1978) 494-497.

14. J.A. Switzer, M.G. Shumsky, E.W. Bohannan, Science 284 (1999) 293-296.

15. P. Shuk, H.D. Wiemhofer, U. Guth, W. Gopel, M. Greenblatt, Solid State Ionics 89 (1996) 179-196

4381 | P a g e
O c t o b e r 2 0 1 6
w w w . c i r w o r l d . c o m

16. B.J. Yang, M.S. Mo, H.M. Hu, C. Li, X.G. Yang, Q.W. Li, Y.T. Qian, Eur. J. Inorg. Chem. 9 (2004) 1785- 1787.

17. C.C. Huang, L.C. Leu, K.Z. Fung, Electrochem. Solid-State Lett. 8 (2005) A204- A206.

18. H. Maeda, N. Tomita, H. Kumakura, K. Togano, Y. Tanaka, Mater. Chem. Phys. 40 (1995) 298-302

19. X.L. Chen, W. Eysel, J. Solid State Chem. 127 (1996) 128-130.

20. A.T. Liu, P. Kleinschmidt, R.W. Davidge (Eds.), Novel Ceramic Fabrication Process and Applications, vol. 38, Institute of Ceramics, Staffs, UK, 1986, pp. 1–10.

21. R.K. Jha, R. Pasricha, V. Ravi, Ceram. Int. 31 (2005) 495-497.

22. L. Madler, S.E. Pratsinis, J. Am. Ceram. Soc. 85 (2002) 1713-1718.

23. M.M. Patil, V.V. Deshpande, S.R. Dhage, V. Ravi, Mater. Lett. 59 (2005) 2523-2525

24. N. Yamazoe, N. Miura, J. Tamaki, Advanced Materials '93, II Vol. 15A, p. 111-116.

25. G.S. Devi, S.V. Manorama, V.J. Rao, Sens. Actuators B 56 (1999) 98-105.

26. T. Hyodo, E. Kanazawa, Y. Takao, Y. Shimizu, M. Egashira, Electrochemistry 68 (2000) 24-31.

27. A.A. Tomchenko, Sens. Actuators B 68 (2000) 48-52.

28. E.L. Shoemaker, C.-U. Kim, M.C. Vogt, Sens. Actuators B 110 (2005) 89-100.

29. S.D. Kapse, F.C. Raghuwanshi, V.D. Kapse, D.R. Patil, Current Applied Physics 12 (2012) 307-312.

30. N.T. G.enov, S. P. Yordanov, "Ceramic Sensors: Technology and Applications", Technomic Pub. Lancaster, 1996, pp. 134-145.

31. A. Gurlo, R. Riedel, Angew. Chem. Int. Ed. 46 (2007) 3826- 3848.

32. J. Zhang, J. Liu, Q. Peng, X. Wang, Y.D. Li, Chem. Mater. 18 (2006) 867- 871.

33. K.J. Albert, N.S. Lewis, C.L. Schauer, G.A. Sotzing, S.E. Stitzel, T.P. Vaid, D.R. Walt, Chem. Rev. 100 (2000) 2595-2626.